Structure−Activity Relationships of Acetylcholinesterase Noncovalent Inhibitors Based on a Polyamine Backbone. 4. Further Investigation on the Inner Spacer

Vincenzo Tumiatti,*[,†,§] Andrea Milelli,[†] Anna Minarini,[†] Michela Rosini,[†] Maria Laura Bolognesi,[†] Marialuisa Micco,[†] Vincenza Andrisano,[†] Manuela Bartolini,[†] Francesca Mancini,[†] Maurizio Recanatini,[†] Andrea Cavalli,[†] and Carlo Melchiorre[†]

Department of Pharmaceutical Sciences, Alma Mater Studiorum, University of Bologna, Via Belmeloro 6, 40126 Bologna, Italy, and Polo Scientifico-Didattico di Rimini, University of Bologna, 40100 Bologna, Italy

Received July 31, 2008

Novel multi-target-directed ligands were designed by replacing the inner dipiperidino function of **3** with less flexible or completely rigid moieties to obtain compounds endowed with multiple biological properties that might be relevant to Alzheimer's disease. **15** was the most interesting, inhibiting AChE in the nanomolar range and inhibiting AChE-induced and self-promoted β-amyloid aggregation in the micromolar range.

Introduction

Alzheimer's disease (AD[a]) is a multifactorial disease and age-related neurodegenerative disorder clinically characterized by loss of memory and progressive deficits in different cognitive domains. Most currently prescribed AD drugs aim to increase the level of acetylcholine (ACh) in the brain by inhibiting AChE. But clinical experience shows that cholinesterases inhibition is a palliative treatment, which does not address AD's etiology.[1] Research into newer and more potent AChE inhibitors (AChEIs) is thus focused on compounds whose properties go beyond AChE inhibition.[2−4]

The "one-molecule−multiple-targets" paradigm suggests that a single molecule could hit several targets responsible for the onset and/or progression of AD.[5,6] To this end, the design and synthesis of multi-target-directed ligands (MTDLs) useful for combating neurodegenerative diseases[6] have been published.[7] This seems more appropriate for addressing the complexity of AD and may provide new drugs for tackling the multifactorial nature of AD, stopping its progression.

In 1998, we reported on derivatives displaying affinity for (i) AChE active and peripheral binding sites and (ii) muscarinic M_2 receptors.[8] The prototypes caproctamine (**1**) and its ethyl analogue (**2**)[9] antagonized muscarinic M_2 receptors and inhibited active and peripheral sites of AChE. Because AChE may act as a chaperone in inducing β-amyloid (Aβ) aggregation through the interaction of its peripheral anionic site (PAS) with the peptide, the inhibition of PAS might be relevant to the search for AChEIs endowed with Aβ antiaggregating properties.[10] Although **1** and **2** contacted PAS and active AChE binding sites, they did not inhibit the AChE-induced Aβ aggregation. To verify whether this failure was due to their high structural flexibility, their inner octamethylene spacer was partially or totally incorporated into a more constrained moiety.[11] This led to the discovery of the dipiperidino derivative **3**, which displayed improved AChE inhibitory potency and the ability to partially inhibit AChE-induced Aβ aggregation, suggesting that inhibition of Aβ aggregation is achieved by polyamines incorporating a constrained spacer between the two inner nitrogen atoms rather than a flexible polymethylene chain.[11] It is known that aromatic residues may give additional interactions with the aromatic rings lined in AChE gorge[12] and may confer β-sheet-breaking properties that might lead to the inhibition of self-mediated Aβ aggregation.[13]

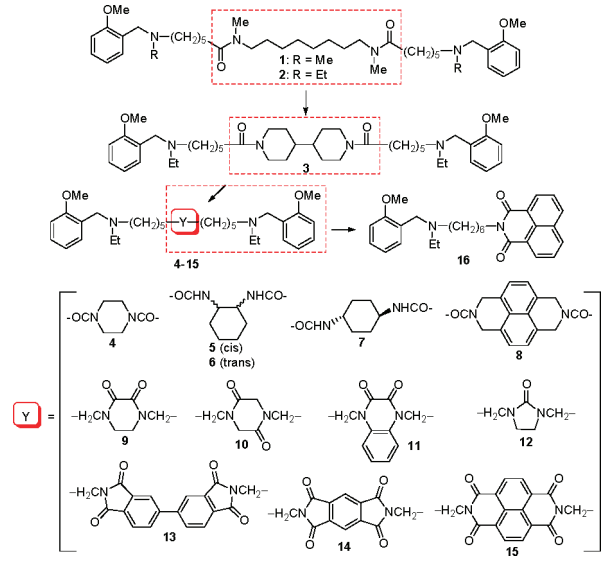

Figure 1. Design strategy for **4**−**16**.

Thus, to obtain new AChE-inhibiting MTDLs endowed with additional properties such as inhibition of AChE-induced Aβ aggregation and β-sheet-breaking ability,[14] we replaced the dipiperidino moiety of **3** with less flexible cyclic systems, leading to **4**−**16** (Figure 1). Monoamine **16** was included in this study to verify the importance, if any, of the two aminoalkyl side chains in the interaction with AChE and Aβ.

Chemistry

Diamine diamides **17**−**21** were obtained by reacting *N*-[(benzyloxy)carbonyl]-6-aminocaproic acid with piperazine, *cis*-cyclohexane-1,2-diamine, (±)-*trans*-cyclohexane-1,2-diamine, *trans*-cyclohexane-1,4-diamine, and ethane-1,2-diamine, respectively. Removal of the *N*-(benzyloxy)carbonyl group by acidic hydrolysis gave diamine diamides **22**−**26**, which were treated

* To whom correspondence should be addressed. Address: Department of Pharmaceutical Sciences, University of Bologna, Via Belmeloro 6, 40126 Bologna, Italy. Phone: +39-051-2099709. Fax: +39-051-2099734. E-mail: vincenzo.tumiatti@unibo.it.

† Department of Pharmaceutical Sciences, University of Bologna.

§ Polo Scientifico-Didattico di Rimini, University of Bologna.

[a] Abbreviations: Aβ, β-amyloid; ACh, acetylcholine; AChE, acetylcholinesterase; AChEI, acetylcholinesterase inhibitor; AD, Alzheimer's disease; BChE, butyrylcholinesterase; MTDL, multi-target-directed ligand; NTD, 1,4,5,8-naphthalenetetracarboxylic diimide; PAS, peripheral anionic site.

10.1021/jm8009684 CCC: $40.75
Published on Web 10/28/2008

Scheme 1[a]

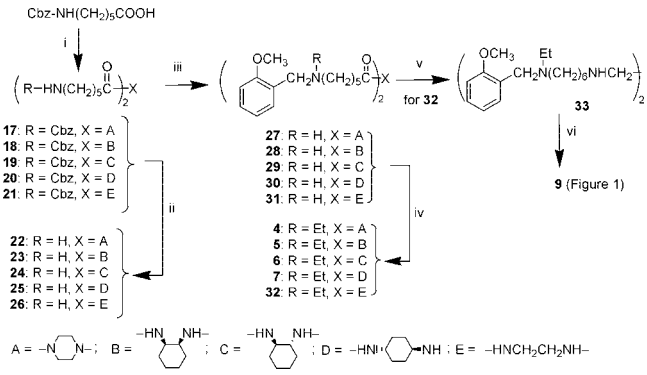

[a] Conditions: Cbz = $C_6H_5CH_2OCO-$; (i) Et_3N, EtOCOCl, dioxane, room temp, 72 h, 49−93%; (ii) 30% HBr in CH_3COOH, CH_3COOH, room temp, 4 h, quantitative yield; (iii) (a) 2-$MeOC_6H_4CHO$, toluene, reflux, 6 h; (b) $NaBH_4$, EtOH, room temp, 6 h, 65−84%; (iv) $(EtO)_2SO_2$, toluene, reflux, 48 h, 26−54%; (v) (a) borane-*N*-ethyl-*N*-isopropylaniline complex, diglyme, reflux, 4 h; (b) 6 N HCl, reflux, 1 h, 23%; (vi) diethyloxalate, EtOH, reflux, 12 h, 42%.

Scheme 2[a]

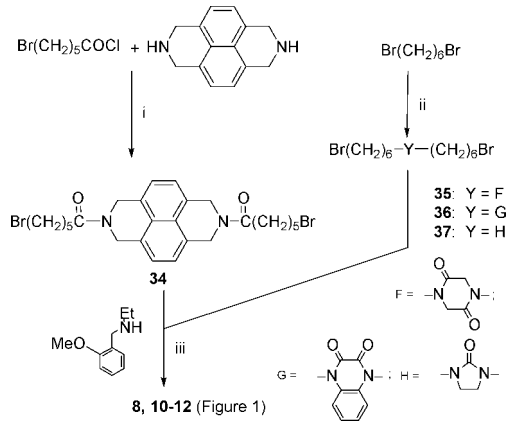

[a] Conditions: (i) Et_3N, CH_2Cl_2, room temp, 96 h, 9%; (ii) 60% NaH, anhydrous DMF, piperazine-2,5-dione or 1,4-dihydroquinoxaline-2,3-dione or imidazolidin-2-one, room temp for **35** and **36** and reflux for **37**, 24 h, 18−46%; (iii) for **10** and **11**, KI, K_2CO_3, 1-pentanol, reflux, 40 h, 11−57%; for **8** and **12**, CH_3CN and Et_3N, reflux, 64 h, 27−30%.

with 2-methoxybenzaldehyde followed by reduction with $NaBH_4$ of the formed Schiff base to the corresponding dibenzyl derivatives **27**−**31**. Diethylation of **27**−**31** with diethyl sulfate gave **4**−**7** (Figure 1) and **32**. Reduction of **32** afforded **33**, which was condensed with diethyloxalate to give **9** (Scheme 1). Acylation of 1,2,3,6,7,8-hexahydrobenzo[*lmn*][3,8]phenanthroline[15] with 6-bromohexanoyl chloride gave **34**, whereas N-alkylation of piperazine-2,5-dione, 1,4-dihydroquinoxaline-2,3-dione, and imidazolidin-2-one with the appropriate dibromoderivative afforded intemediates **35**−**37**, which were diaminated with ethyl-(2-methoxybenzyl)amine to give **8**, **10**−**12** (Figure 1), respectively (Scheme 2).

Finally, **13**−**16** (Figure 1) were obtained through the condensation of the commercially available anhydrides [5,5′]biisobenzofuranyl-1,3,1′,3′-tetraone, benzo[1,2-*c*;4,5-*c*′]difuran-1,3,5,7-tetraone, isochromeno[6,5,4-*def*]isochromene-1,3,6,8-tetraone, and benzo[*de*]isochromene-1,3-dione, respectively, with *N*-ethyl-*N*-(2-methoxybenzyl)hexane-1,6-diamine[16] (Scheme 3). Different salts (dioxalates for **4**−**10**, **12**, and **15** and di-*p*-

Scheme 3[a]

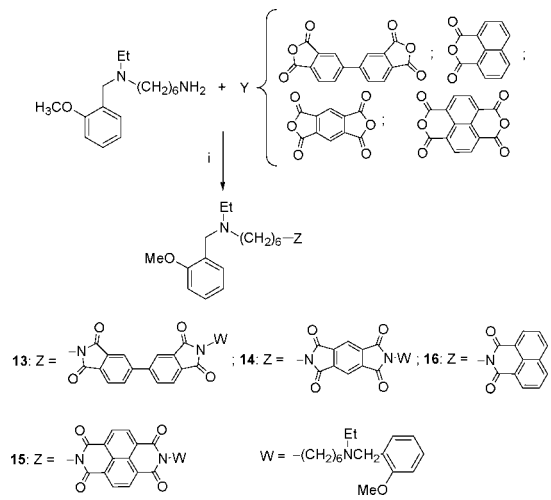

[a] Conditions: (i) amine and anhydride molar ratio, 2:1 for **13**−**15** and 1:1 for **16**, EtOH, reflux, 60 h, 35−51%.

toluenesulfonates for **11**−**14**) were prepared to obtain derivatives easier to handle.

Results and Discussion

To determine the potential interest of **4**−**16** for AD treatment, their inhibitory potency was evaluated on recombinant human AChE and isolated BChE from human serum in comparison with polyamines **1**−**3** and the marketed drugs donepezil and galantamine.

An analysis of the results (Table 1) reveals that replacement of the dipiperidino moiety of **3** with constrained moieties strongly influenced the ability to inhibit AChE and BChE. The new derivatives inhibited AChE activity in the nanomolar range with the exception of **5**−**7**. The low affinity of **5**−**7** for AChE might be due to the difficulty of the two amide functions to assume a planar arrangement to each other, as is probably possible for **4**, **9**, **10**, and **12**, which were only slightly less potent than **3**. The most potent compounds of the present series (**8**, **11**, **13**−**15**) were characterized by an aromatic residue in the middle of their structure. This suggests the possibility of establishing more $\pi-\pi$ interactions with several aromatic residues located in the AChE gorge. In particular, **15**, endowed with a 1,4,5,8-naphthalenetetracarboxylic diimide (NTD) moiety, showed a very high AChE inhibitory activity and a 9-fold improvement in potency in comparison with **3**. All the synthesized compounds showed a selective inhibitory activity for AChE relative to BChE, and **15** was the most selective and potent of the series with an AChE/BChE selectivity ratio greater than 5000, perhaps relevant when considering the emerging role of BChE in AD[17] and the importance of selectivity toward AChE in AD treatment.[18] Finally, **16**, characterized by only one side chain, was 144-fold less potent than **15**, highlighting the importance of the presence of two side chains for an optimal interaction with both sites of AChE.

PAS is well-established as important for Aβ-fibrils formation mediated by AChE;[10,19] thus, compounds able to interact with amino acids located in the PAS area may reduce the formation of neurotoxic Aβ fibrils. PAS may thus be an attractive target when developing potential AD-modifying drugs. A Lineweaver−Burk plot obtained at increasing concentrations of substrate and inhibitor showed that **15** interacted with the catalytic site and PAS (see Supporting Information). Therefore, the ability of **4** and **7**−**16** to inhibit AChE-induced Aβ(1−40)

Table 1. Inhibition of AChE and BChE Activities and of AChE-Mediated and Self-Induced Aβ Aggregation by **4**−**16** and Reference Polyamines **1**−**3**

	IC_{50} (nM)[b]		inhibition of Aβ aggregation (%)	
compd[a]	AChE	BChE	AChE-induced[c]	self-induced[d]
1[e]	170 ± 2[e]	11600 ± 300[e]	<5[f]	20.3 ± 1.9
2	16.1 ± 0.5[e]	2250 ± 60[e]	<5	nd[h]
3	3.32 ± 0.12[g]	8490 ± 610[g]	41.2 ± 2.0	13.7 ± 6
4	25.7 ± 1.9	10700 ± 1900	38.9 ± 4.0	<5[f]
5	4160 ± 200	30800 ± 2300	nd[h]	nd[h]
6	5470 ± 240	36800 ± 3300	nd[h]	nd[h]
7	8550 ± 40	25300 ± 4200	25.6 ± 4.6	nd[h]
8	4.83 ± 0.16	1040 ± 30	42.1 ± 2.2	12.7 ± 2.9
9	68.9 ± 2.4	10300 ± 400	47.5 ± 1.6	nd[h]
10	15.9 ± 0.6	2090 ± 130	61.4 ± 4.4	4.8 ± 1.3
11	1.41 ± 0.03	95.8 ± 1.5	70.8 ± 3.2	8.8 ± 2.9
12	72.4 ± 3.2	876 ± 24	53.8 ± 3.7	<5
13	14.0 ± 0.6	293 ± 23	70.2 ± 4.83	16.5 ± 1.3
14	7.70 ± 0.27	3000 ± 200	51.1 ± 0.3	<5
15	0.37 ± 0.02	1910 ± 120	>90[i]	54.5 ± 5.4[j]
16	53.5 ± 5.7	416 ± 32	19.5 ± 2.8	<5
donepezil	23.1 ± 4.8	7420 ± 390	22[k]	<5
galantamine	2010 ± 150[l]	20700 ± 1500[l]	17.9 ± 0.1[l]	<5
propidium	32300[l]	13200[l]	82.0 ± 2.5[k]	61.1 ± 4.6[l]
Congo red	nd[h]	nd[h]	nd[h]	78.8 ± 0.9[l]

[a] **1**, dihydrochloride; **2**−**10**, **12**, and **15**, dioxalate; **11**, **13**, **14**, di-*p*-toluenesulfonate; **16**, *p*-toluenesulfonate. See Figure 1 for structures. [b] Human recombinant AChE and BChE from human serum were used. IC_{50} values represent the concentration of inhibitor required to decrease enzyme activity by 50% and are the mean of two independent measurements, each performed in triplicate. [c] Inhibition of AChE-induced Aβ(1−40) aggregation. The concentrations of the tested inhibitor and Aβ(1−40) were 100 and 230 μM, respectively, whereas the Aβ(1−40)/AChE ratio was equal to 100:1. [d] Inhibition of self-induced Aβ(1−42) aggregation (50 μM) produced by the tested compound at 10 μM concentration. [e] Data from ref 8. [f] Not significant. [g] Data from ref 30. [h] nd, not determined. [i] $IC_{50} = 8.13 \pm 0.97$ μM. [j] $IC_{50} = 9.69 \pm 1.09$ μM. [k] Data from ref 10. [l] Data from ref 24.

aggregation was assessed through a thioflavin T-based fluorometric assay.[10] **5** and **6** were not evaluated because of their poor AChE inhibitory activity. **4**, **8**, and **9** were as active as **3** (Table 1), while **10**−**15** were more potent than **3**. It appears that an inner spacer bearing aromatic residues may be optimal for inhibiting AChE-induced Aβ aggregation. **15** was the most potent inhibitor with an IC_{50} lower than that of the reference compound propidium.[10] Notably, neither **3** nor any of the marketed AChE inhibitors, when tested in the same conditions, showed comparable antiaggregating activity.[10,20] The most potent published compounds acting as AChE-induced Aβ aggregation inhibitors display a potency in the same range as **15**.[21−23] The low inhibitory activity shown by **16** emphasizes the importance of the two aminoalkyl side chains for an optimal interaction with the two AChE binding sites.

Since it was previously reported that compounds endowed with a polyamine scaffold may interfere with Aβ polymerization and aggregation,[24] the ability of **4**, **8**, **10**−**16** to inhibit self-promoted Aβ(1−42) aggregation was also determined (Table 1).[10] Again, **15**, although less potent that the reference compound Congo red, displayed an IC_{50} comparable with that of propidium. This activity might be due to the ability of **15** to behave as a β-sheet breaker because of its planar and constrained aromatic system.[19] Unfortunately, because of its low solubility, the contribution, if any, of the NTD moiety benzo[*lmn*][3,8]phenanthroline-1,3,6,8-tetraone[15] and, consequently, its possible contribution to the different biological properties of **15** could not be determined.

To disclose a possible binding mode of **15** at AChE and BChE binding pockets, docking simulations were performed using the available crystallographic structures of the two enzymes (PDB codes: 1B41 for AChE,[25] 1P0M for BChE[26]). Because of **15**'s flexibility, several docking runs were carried out with GOLD.[27] The outcomes were clusterized by AClAP.[28] In Figure 2SI of Supporting Information, a low energy pose representative of a statistically populated cluster is reported for binary complexes of AChE and **15** (Figure 2A of Supporting Information) and of BChE and **15** (Figure 2B of Supporting Information). The binding mode of **15** at the AChE gorge shows that the ligand can interact with Trp86 of the internal anionic site and with Trp286 of PAS (Figure 2A of Supporting Information). The latter could explain **15**'s ability to inhibit AChE-induced Aβ aggregation. **15** might also interact with several aromatic residues of the enzyme mid-gorge.[29] In particular, the NTD moiety could establish favorable $\pi-\pi$ stacking or simple hydrophobic interactions with Tyr341, Phe338, and Phe295. Moreover, Tyr72 may interact by H-bonding with the methoxy substituent of one of the benzylammonium ends. This could account for the high inhibitory potency of **15** against human AChE. Conversely, although **15** could favorably interact with several BChE amino acids (Figure 2B of Supporting Information), the lack of the same pool of aromatic residues at the BChE mid-gorge may explain **15**'s AChE/BChE selectivity. Indeed, besides a cation$-\pi$ interaction between **15** and the Trp82 indole ring of BChE, the only other striking interaction was between **15** and Tyr332. Moreover, **15** seemed unable to interact with Phe278, a fundamental residue for inhibiting BChE activity.[29] The presence of BChE Asp70 close to one of the two imide moieties of the NTD scaffold may further decrease the molecule's affinity toward this target.

Conclusions

We have demonstrated that constraining the dipiperidino moiety of **3** led to derivatives with a better biological profile. The most potent was **15**, endowed with an NTD moiety. It inhibited AChE in the subnanomolar range and inhibited AChE-induced and self-promoted Aβ aggregation in micromolar concentration. Thus, **15** emerges as an MTDL able to hit several targets of the AD pathogenesis cascade.

However, the rational design of compounds that simultaneously modulate different protein targets at a comparable concentration for each target remains a challenging task.[6] In the present case, proof of the concept of the biological profile of **15** in vivo is needed to confirm the relevance of the NTD moiety in the design of new derivatives for AD treatment.

Experimental Section

General Procedure for the Synthesis of 4−7. A mixture of **27**, **28**, **29**, or **30** and diethyl sulfate (1:2.5 ratio) was heated at the refluxing temperature for 48 h in toluene. After removal of the solvent, the residue was taken up in water, made basic with KOH pellets, and immediately extracted with $CHCl_3$ (3 × 20 mL) or directly purified by column chromatography to avoid quaternarization of amine functions. Removal of the dried solvent gave a residue that was purified by gravity chromatography, providing the desired **4**−**7**, which were converted into the corresponding dioxalate salts by adding 2 equiv of oxalic acid in ether to an ether solution of the free base. See Supporting Information for further experimental details, elemental analysis (EA) data, and spectral data (ESI-MS and ^1H and ^{13}C NMR).

General Procedure for the Synthesis of 8 and 12. A mixture of ethyl(2-methoxybenzyl)amine (0.125 g, 0.76 mmol) and triethylamine (0.077 g, 0.76 mmol) was added to a solution of the dibromo derivative **34** or **37** (0.38 mmol) in CH_3CN (20 mL). The reaction mixture was stirred at the refluxing temperature for 64 h. After solvent evaporation, the crude material was poured in water, made basic, and extracted with CH_2Cl_2 (3 × 50 mL). After evaporation

of the solvent, the crude material was purified by flash chromatography. The two purified compounds were converted into the dioxalate salts as described for **4**−**7**.

8. It was synthesized from **34**: yellow oil; 27% yield; eluting solvent, toluene/EtOAc/MeOH/CH_2Cl_2/aqueous 33% ammonia (4:4:1:1:0.05); ^{1}H NMR (free base, 200 MHz, $CDCl_3$) δ 1.01 (t, J = 5.4, 6H), 1.17−1.68 (m, 12H), 1.68−2.51 (m, 12H), 3.38 (s, 6H), 3.58 (s, 4H), 4.88 (s, 4H), 5.06 (s, 4H), 6.68−6.96 (m, 4H), 7.17−7.42 (m, 8H); ^{13}C NMR (200 MHz, $CDCl_3$) δ 11.9, 25.3, 27.0, 27.5, 44.7, 47.8, 48.8, 51.4, 53.5, 55.4, 110.3, 120.3, 127.6, 127.9, 128.2, 130.2, 157.7, 198.1; MS (ESI$^+$) m/z = 733 $(M + H)^+$. Anal. ($C_{50}H_{64}N_4O_{12}$), C, H, N.

12. See Supporting Information for further experimental details, EA, and spectral data (ESI-MS and ^{1}H and ^{13}C NMR).

General Procedure for the Synthesis of 10 and 11. KI (1.6 g, 10 mmol), K_2CO_3 (4.7 g, 17 mmol), and ethyl(2-methoxybenzyl)amine (0.313 g, 1.9 mmol) were added to a solution of the dibromoderivative **35** or **36** (0.38 mmol) in *n*-pentanol (20 mL). The resulting mixture was heated at the refluxing temperature for 40 h. After evaporation of the solvent the crude product was washed with water and taken up with a 1:1 mixture of ether and ethyl acetate (50 mL). The organic phase was dried and the solvent evaporated. The crude mixture was purified by flash chromatography to afford the desired compound. **10** was converted into the dioxalate salt as described for **4**−**7**, and **11** was converted into the di-*p*-toluenesulfonate salt by adding 2 equiv of *p*-toluenesulfonic acid in ether to an ether solution of the free base.

10. See Supporting Information for further experimental details, EA, and spectral data (ESI-MS and ^{1}H and ^{13}C NMR).

11. It was synthesized from **36**: yellow oil; 11% yield; eluting solvent, toluene/EtOAc/MeOH/ aqueous 33% ammonia (4:5:1:0.03); ^{1}H NMR (free base, 200 MHz, $CDCl_3$) δ 1.07 (t, J = 6.0, 6H), 1.38−1.77 (m, 16H), 2.50 (t, J = 15, 4H), 2.55 (q, J = 7.5, 4H), 3.61 (s, 4H), 3.83 (s, 6H), 4.19 (t, J = 7.8, 4H), 6.85−7.44 (m, 12H); ^{13}C NMR (200 MHz, $CDCl_3$) δ 11.7, 26.8, 26.9, 43.2, 47.6, 51.3, 53.2, 55.3, 110.2, 115.1, 120.3, 124.0, 126.7, 127.6, 130.1, 151.0, 154.1, 157.6; MS (ESI$^+$) m/z = 657 $(M + Na)^+$. Anal. ($C_{54}H_{72}N_4O_{10}S_2$) C, H, N.

Synthesis of 9. See Supporting Information.

General Procedure for the Synthesis of 13−16. A solution of *N*1-ethyl-*N*1-(2-methoxybenzyl)hexane-1,6-diamine[16] (0.08 mmol, for **16** 0.04 mmol) and the appropriate anhydride (0.4 mmol) in ethanol (40 mL) was heated at the refluxing temperature for 60 h. After the mixture was cooled to room temperature, the solvent was evaporated to give a crude material which was purified by flash chromatography. **13** and **14** were converted into the di-*p*-toluenesulfonate salts, whereas **15** and **16** were converted into the dioxalate and *p*-toluenesulfonate salt, respectively.

13, 14, 16. See Supporting Information for further experimental details, EA, and spectral data (ESI-MS and ^{1}H and ^{13}C NMR).

15. It was synthesized from isochromeno[6,5,4-*def*]isochromene-1,3,6,8-tetraone: colorless oil; 43% yield; eluting solvent, toluene/EtOAc/CH_2Cl_2/MeOH/aqueous 33% ammonia (4:4:1:1:0.05); ^{1}H NMR (free base, $CDCl_3$) δ 1.05 (t, J = 7.4, 6H), 1.43−1.76 (m, 16H), 2.43−2.59 (m, 8H), 3.58 (s, 4H), 3.82 (s, 6H), 4.19 (t, J = 7.6, 4H), 6.18−6.96 (m, 4H), 7.15−7.28 (m, 2H), 7.89−7.43 (m, 2H), 8.77 (s, 4H); ^{13}C NMR (free base, $CDCl_3$) δ 1.12, 11.96, 27.07 27.16, 27.37, 28.22, 41.02, 47.74, 51.44, 53.58, 55.41, 110.25, 120.35, 125.38, 126.69, 127.52, 128.29, 128.40, 129.10, 130.13, 130.94, 157.73, 162.85; MS (ESI$^+$) m/z = 761 $(M + H)^+$. Anal. ($C_{50}H_{60}N_4O_{14}$) C, H, N.

Acknowledgment. The authors thank Valeria Battelli, Massimo Gambuti, Marianna Leardini, and Elisa Piersanti for technical assistance. This research was supported by a grant from MIUR, Rome (PRIN), and Polo Scientifico-Didattico di Rimini.

Supporting Information Available: Experimental details for chemistry, biology, and modeling; elemental analysis data of target compounds; and experimental details and characterization of intermediate compounds. This material is available free of charge via the Internet at http://pubs.acs.org.

References

(1) Cummings, J. L.; Doody, R.; Clark, C. Disease-modifying therapies for Alzheimer disease: challenges to early intervention. *Neurology* **2007**, *69*, 1622–1634.
(2) Relkin, N. R. Beyond symptomatic therapy: a re-examination of acetylcholinesterase inhibitors in Alzheimer's disease. *Expert Rev. Neurother.* **2007**, *7*, 735–748.
(3) Holzgrabe, U.; Kapkova, P.; Alptuzun, V.; Scheiber, J.; Kugelmann, E. Targeting acetylcholinesterase to treat neurodegeneration. *Expert Opin. Ther. Targets* **2007**, *11*, 161–179.
(4) Martinez, A.; Castro, A. Novel cholinesterase inhibitors as future effective drugs for the treatment of Alzheimer's disease. *Expert Opin. Invest. Drugs* **2006**, *15*, 1–12.
(5) Van der Schyf, C. J.; Geldenhuys, W. J.; Youdim, M. B. Multifunctional drugs with different CNS targets for neuropsychiatric disorders. *J. Neurochem.* **2006**, *99*, 1033–1048.
(6) Cavalli, A.; Bolognesi, M. L.; Minarini, A.; Rosini, M.; Tumiatti, V.; Recanatini, M.; Melchiorre, C. Multi-target-directed ligands to combat neurodegenerative diseases. *J. Med. Chem.* **2008**, *51*, 347–372.
(7) Decker, M. Recent advances in the development of hybrid molecules/designed multiple compounds with antiamnesic properties. *Mini-Rev. Med. Chem.* **2007**, *7*, 221–229.
(8) Melchiorre, C.; Andrisano, V.; Bolognesi, M. L.; Budriesi, R.; Cavalli, A.; Cavrini, V.; Rosini, M.; Tumiatti, V.; Recanatini, M. Acetylcholinesterase noncovalent inhibitors based on a polyamine backbone for potential use against Alzheimer's disease. *J. Med. Chem.* **1998**, *41*, 4186–4189.
(9) Tumiatti, V.; Rosini, M.; Bartolini, M.; Cavalli, A.; Marucci, G.; Andrisano, V.; Angeli, P.; Banzi, R.; Minarini, A.; Recanatini, M.; Melchiorre, C. Structure−activity relationships of acetylcholinesterase noncovalent inhibitors based on a polyamine backbone. 2. Role of the substituents on the phenyl ring and nitrogen atoms of caproctamine. *J. Med. Chem.* **2003**, *46*, 954–966.
(10) Bartolini, M.; Bertucci, C.; Cavrini, V.; Andrisano, V. beta-Amyloid aggregation induced by human acetylcholinesterase: inhibition studies. *Biochem. Pharmacol.* **2003**, *65*, 407–416.
(11) Tumiatti, V.; Andrisano, V.; Banzi, R.; Bartolini, M.; Minarini, A.; Rosini, M.; Melchiorre, C. Structure−activity relationships of acetylcholinesterase noncovalent inhibitors based on a polyamine backbone. 3. Effect of replacing the inner polymethylene chain with cyclic moieties. *J. Med. Chem.* **2004**, *47*, 6490–6498.
(12) Axelsen, P. H.; Harel, M.; Silman, I.; Sussman, J. L. Structure and dynamics of the active site gorge of acetylcholinesterase: synergistic use of molecular dynamics simulation and X-ray crystallography. *Protein Sci.* **1994**, *3*, 188–197.
(13) Nesterov, E. E.; Skoch, J.; Hyman, B. T.; Klunk, W. E.; Bacskai, B. J.; Swager, T. M. In vivo optical imaging of amyloid aggregates in brain: design of fluorescent markers. *Angew. Chem., Int. Ed.* **2005**, *44*, 5452–5456.
(14) Adessi, C.; Soto, C. Beta-sheet breaker strategy for the treatment of Alzheimer's disease. *Drug Dev. Res.* **2002**, *56*, 184–193.
(15) Sotiriou-Leventis, C.; Mao, Z. A facile synthesis of 2,7-diazapyrene. *J. Heterocycl. Chem.* **2000**, *37*, 1665–1667.
(16) Cavalli, A.; Bolognesi, M. L.; Capsoni, S.; Andrisano, V.; Bartolini, M.; Margotti, E.; Cattaneo, A.; Recanatini, M.; Melchiorre, C. A small molecule targeting the multifactorial nature of Alzheimer's disease. *Angew. Chem., Int. Ed.* **2007**, *46*, 3689–3692.
(17) Diamant, S.; Podoly, E.; Friedler, A.; Ligumsky, H.; Livnah, O.; Soreq, H. Butyrylcholinesterase attenuates amyloid fibril formation in vitro. *Proc. Natl. Acad. Sci. U.S.A.* **2006**, *103*, 8628–8633.
(18) Liston, D. R.; Nielsen, J. A.; Villalobos, A.; Chapin, D.; Jones, S. B.; Hubbard, S. T.; Shalaby, I. A.; Ramirez, A.; Nason, D.; White, W. F. Pharmacology of selective acetylcholinesterase inhibitors: implications for use in Alzheimer's disease. *Eur. J. Pharmacol.* **2004**, *486*, 9–17.
(19) Inestrosa, N. C.; Alvarez, A.; Perez, C. A.; Moreno, R. D.; Vicente, M.; Linker, C.; Casanueva, O. I.; Soto, C.; Garrido, J. Acetylcholinesterase accelerates assembly of amyloid-beta-peptides into Alzheimer's fibrils: possible role of the peripheral site of the enzyme. *Neuron* **1996**, *16*, 881–891.
(20) Bolognesi, M. L.; Bartolini, M.; Cavalli, A.; risano, V.; Rosini, M.; Minarini, A.; Melchiorre, C. Design, synthesis, and biological evaluation of conformationally restricted rivastigmine analogues. *J. Med. Chem.* **2004**, *47*, 5945–5952.
(21) Munoz-Ruiz, P.; Rubio, L.; Garcia-Palomero, E.; Dorronsoro, I.; del Monte-Millan, M.; Valenzuela, R.; Usan, P.; de Austria, C.; Bartolini, M.; Andrisano, V.; Bidon-Chanal, A.; Orozco, M.; Luque, F. J.; Medina, M.; Martinez, A. Design, synthesis, and biological evaluation of dual binding site acetylcholinesterase inhibitors: new disease-

modifying agents for Alzheimer's disease. *J. Med. Chem.* **2005**, *48*, 7223–7233.

(22) Xie, Q.; Wang, H.; Xia, Z.; Lu, M.; Zhang, W.; Wang, X.; Fu, W.; Tang, Y.; Sheng, W.; Li, W.; Zhou, W.; Zhu, X.; Qiu, Z.; Chen, H. Bis-(−)-nor-meptazinols as novel nanomolar cholinesterase inhibitors with high inhibitory potency on amyloid-beta aggregation. *J. Med. Chem.* **2008**, *51*, 2027–2036.

(23) Bolognesi, M. L.; risano, V.; Bartolini, M.; Banzi, R.; Melchiorre, C. Propidium-based polyamine ligands as potent inhibitors of acetylcholinesterase and acetylcholinesterase-induced amyloid-beta aggregation. *J. Med. Chem.* **2005**, *48*, 24–27.

(24) Bolognesi, M. L.; Banzi, R.; Bartolini, M.; Cavalli, A.; Tarozzi, A.; risano, V.; Minarini, A.; Rosini, M.; Tumiatti, V.; Bergamini, C.; Fato, R.; Lenaz, G.; Hrelia, P.; Cattaneo, A.; Recanatini, M.; Melchiorre, C. Novel class of quinone-bearing polyamines as multi-target-directed ligands to combat Alzheimer's disease. *J. Med. Chem.* **2007**, *50*, 4882–4897.

(25) Kryger, G.; Harel, M.; Giles, K.; Toker, L.; Velan, B.; Lazar, A.; Kronman, C.; Barak, D.; Ariel, N.; Shafferman, A.; Silman, I.; Sussman, J. L. Structures of recombinant native and E202Q mutant human acetylcholinesterase complexed with the snake-venom toxin fasciculin-II. *Acta Crystallogr., Sect. D: Biol. Crystallogr.* **2000**, *56*, 1385–1394.

(26) Nicolet, Y.; Lockridge, O.; Masson, P.; Fontecilla-Camps, J. C.; Nachon, F. Crystal structure of human butyrylcholinesterase and of its complexes with substrate and products. *J. Biol. Chem.* **2003**, *278*, 41141–41147.

(27) Jones, G.; Willett, P.; Glen, R. C.; Leach, A. R.; Taylor, R. Development and validation of a genetic algorithm for flexible docking. *J. Mol. Biol.* **1997**, *267*, 727–748.

(28) Bottegoni, G.; Cavalli, A.; Recanatini, M. A comparative study on the application of hierarchical-agglomerative clustering approaches to organize outputs of reiterated docking runs. *J. Chem. Inf. Model.* **2006**, *46*, 852–862.

(29) Campiani, G.; Fattorusso, C.; Butini, S.; Gaeta, A.; Agnusdei, M.; Gemma, S.; Persico, M.; Catalanotti, B.; Savini, L.; Nacci, V.; Novellino, E.; Holloway, H. W.; Greig, N. H.; Belinskaya, T.; Fedorko, J. M.; Saxena, A. Development of molecular probes for the identification of extra interaction sites in the mid-gorge and peripheral sites of butyrylcholinesterase (BuChE). Rational design of novel, selective, and highly potent BuChE inhibitors. *J. Med. Chem.* **2005**, *48*, 1919–1929.

(30) Piazzi, L.; Rampa, A.; Bisi, A.; Gobbi, S.; Belluti, F.; Cavalli, A.; Bartolini, M.; Andrisano, V.; Valenti, P.; Recanatini, M. 3-(4-[[Benzyl(methyl)amino]methyl]phenyl)-6,7-dimethoxy-2*H*-2-chromenone (AP2238) inhibits both acetylcholinesterase and acetylcholinesterase-induced beta-amyloid aggregation: a dual function lead for Alzheimer's disease therapy. *J. Med. Chem.* **2003**, *46*, 2279–2282.

JM8009684